# Design of two-helix motifs in peptides: crystal structure of a system of linked helices of opposite chirality and a model helix–linker peptide

Isabella L Karle[1], Arindam Banerjee[2] and Padmanabhan Balaram[2]

**Background**: An attempt is being made to produce two-helix bundles that are soluble in apolar media, without the use of a rigid template. The approach relies on the use of stereochemically constrained amino acids for helix construction, while a flexible linker is obtained by the use of an ϵ-aminocaproic acid residue (Acp). The Acp linker has appropriate NH and COOH termini to connect to the N and C termini of the helices, a flexible $(CH_2)_5$ moiety and sufficient length to make the desired assembly.

**Results**: The conformations in crystals (determined by X-ray diffraction analyses) are described for a partial assembly consisting of a 7-residue helix with Acp (helix–Acp) and for two assemblies of 7-residue helices with Acp (helix–Acp–helix) in which the chiralities of the helices are L,L (already published) and L,D (this publication). The Acp linker is extended away from the helix in the L,L analog in a zig-zag manner, but assumes a helical conformation in the L,D analog. The two helices in the L,L and L,D analogs are displaced laterally by the linker, but in neither case has the linker folded the molecule into the desired U-conformation. Cell parameters for Boc-L-Val-L-Ala-L-Leu-Aib-L-Val-L-Ala-L-Leu-Acp-D-Val-D-Ala-D-Leu-Aib-D-Val-D-Ala-D-Leu-OMe are space group $P4_1$ with $a = b = 10.094(6)$ Å and $c = 93.383(12)$ Å.

**Conclusions**: Strong hydrogen bonds (NH···O=C) between the displaced helices of one molecule and the displaced helices of a neighboring molecule, which form near the linker of each helix–linker–helix assembly, appear to dominate in both the L,L and L,D crystal. The $(CH_2)_5$ segment of the linker readily adopts different conformations that result in the L and D helices packing in a similar spatial motif. Greater conformational control at the linking segment or introduction of specific interhelix interactions may be necessary in order to achieve U-type folding between neighboring helices in a single molecule.

Addresses: [1]Laboratory for the Structure of Matter, Naval Research Laboratory, Washington DC 20375-5341, USA. [2]Molecular Biophysics Unit, Indian Institute of Science, Bangalore 560 012, India.

Correspondence: Isabella L Karle

Key words: Aib peptides, ϵ-aminocaproic acid peptides, left and right handed peptide helices, linker displaced helices, supramolecular assembly

Received: 25 Feb 1997
Revisions requested: 09 Apr 1997
Revisions received: 28 Apr 1997
Accepted: 07 May 1997

Published: 19 Jun 1997
Electronic identifier: 1359-0278-002-00203

Folding & Design 19 Jun 1997, 2:203–210



## Introduction

The formation of compact tertiary structures in peptides and proteins requires stabilizing interactions between residues that are distant in the primary sequence. In natural proteins, solvent-driven hydrophobic interactions facilitate formation of collapsed compact structures, with optimal packing determining the final folded structures [1–3]. *De novo* design approaches [4–6] have attempted to mimic protein folds by using template-assembled secondary structures. The templates used have ranged from cyclic peptides [7–9] and porphyrins [10,11] to metal ions [12–14]. Helical bundles have been the favored target of *de novo* design [15–18]. In the absence of templates, hydrophobically driven clustering has been used to organize amphipathic helical sequences into helix clusters.

An alternative approach to the design of synthetic protein mimics has been extensively investigated in this laboratory in which stereochemically constrained non-protein amino acids are used to construct conformationally robust elements of secondary structures such as helices and β-hairpins [19,20] that are characterizable in crystals. These rigid modules of secondary structures are then connected by short linking segments. This has been termed the 'Meccano set' or 'Lego set' approach to synthetic protein design [19,21]. A large number of structurally well defined modules of secondary structures, both helices [22–25] and hairpins [26,27], have been characterized, ranging in length from 7 to 16 residues. Most of these short sequences have been composed of entirely hydrophobic amino acids resulting in high solubility in organic solvents. We have been investigating the possibility of compact super secondary structure formation facilitated by solvophobic interactions [1,28]. In principle, large apolar faces of molecules must be appreciably solvated in low dielectric constant media. Compaction which results from interactions between large complementary apolar faces should release several solute molecules resulting in an entropically driven close-packed

**Figure 1**

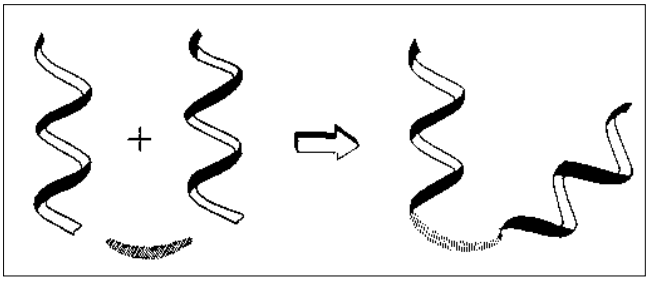

Schematic diagram of a synthetic, approximately U-shaped two-helix motif.

arrangement, entirely analogous to the hydrophobic effects in aqueous solution [1,28,29].

Figure 1 illustrates, schematically, the general principle of the Meccano set approach in constructing linked helix motifs or a two-helix bundle. Construction of helices consisting of 3–4 turns is relatively straightforward, using helix-nucleating α,α-dialkylated amino acids of which α-aminoisobutyric acid (Aib, or U in the one-letter amino acid code) is the prototype [30,31]. Control of helix orientation is a more difficult task. The failure of attempts to use interrupting sequences containing Gly-Pro [32] and D-Phe-Pro [33] segments prompted an investigation of flexible linkers, derived from ω-amino acids. The intention was to use an ϵ-aminocaproic acid residue (Acp) in which the two end moieties, NH and $C^{\alpha}H_2C{=}O$, provide hydrogen bonding groups that serve to continue the helical conformation of the individual helices while the central $(CH_2)_5$ chain provides sufficient flexibility for chain folding as shown in Figure 1. The crystal structure of the model helix–linker–helix Boc-L-Val-L-Ala-L-Leu-Aib-L-Val-L-Ala-L-Leu-Acp-L-Val-L-Ala-L-Leu-Aib-L-Val-L-Ala-L-Leu-OMe reveals an extended arrangement of two distinct helical segments that are laterally displaced with respect to one another (Figure 2) [19]. High-performance liquid chromatography (HPLC) on a hydrophobic C-18 column showed, however, that the synthetic helix–linker–helix peptide has a dramatically lower retention time than a continuous helix of comparable length and sequence [21]. This suggested that compact folded structures with appreciably lower hydrophobic surface areas may, in fact, be populated in solution.

In order to promote compact arrangements and sufficiently close packing of the two helical modules, we have investigated a synthetic sequence in which the two helices have opposing chiral senses. Preliminary modeling studies suggested that close packing of helices connected by short linkers may be facilitated by reversal of helix handedness. The expectation was that favorable helix packing would outweigh intermolecular hydrogen bonding interactions in the

**Figure 2**

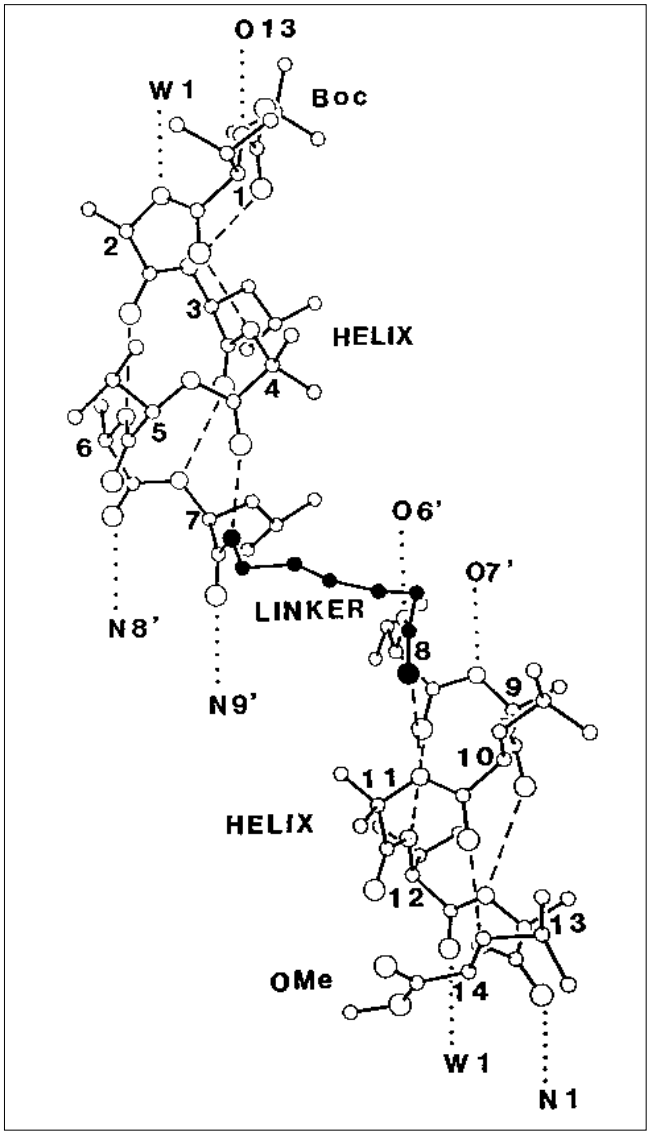


The structure of Boc-L-Val-L-Ala-L-Leu-Aib-L-Val-L-Ala-L-Leu-Acp-L-Val-L-Ala-L-Leu-Aib-L-Val-L-Ala-L-Leu-OMe as determined by crystal structure analysis [19]. Intramolecular NH···O=C bonds in the helices are indicated by dashes. Intermolecular hydrogen bonds are indicated by dots. The atoms in the ϵ-aminocaproic (Acp) linker are shown as filled circles. The water molecule in the head-to-tail region is designated by W1. The $C^{\alpha}$ atoms are numbered 1–14.

crystal that determine the extended arrangement of helices in the all-L peptide. This paper describes the crystal structure of the designed peptide Boc-L-Val-L-Ala-L-Leu-Aib-L-Val-L-Ala-L-Leu-Acp-D-Val-D-Ala-D-Leu-Aib-D-Val-D-Ala-D-Leu-OMe (**2**), in which the N-terminal module comprises L amino acids and the C-terminal module comprises D amino acids — i.e. Boc-L-(VALUVAL)-Acp-D-(VALUVAL)-OMe. In order to further explore the conformational properties of the flexible linker ϵ-aminocaproic

**Figure 3**

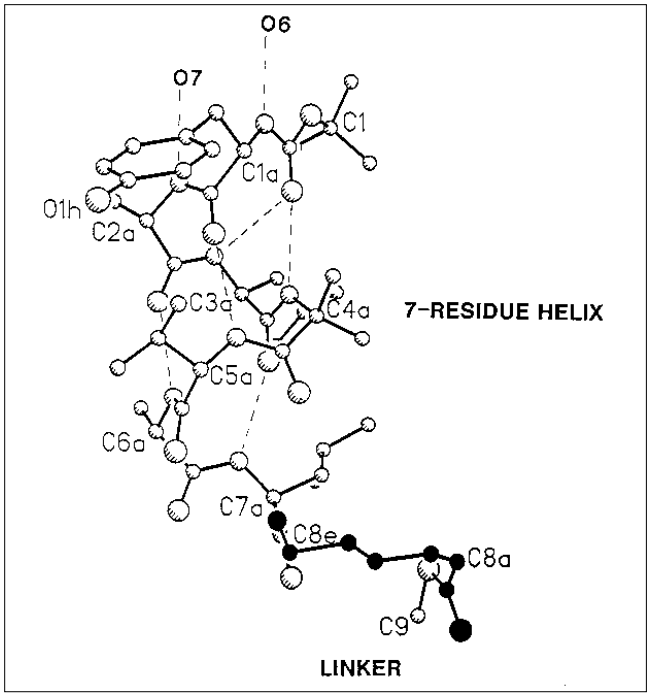


The structure of Boc-L-Tyr-L-(ALUVAL)-Acp-OMe (**1**). Compare to the upper helix and linker in Figure 2.

acid, a structure determination has also been performed for a partial assembly consisting of one helix plus the linker, Boc-L-Tyr-L-Ala-L-Leu-Aib-L-Val-L-Ala-L-Leu-Acp-OMe (**1**) — i.e. Boc-L-Tyr-L-(ALUVAL)-Acp-OMe.

## Results and discussion

### The designed molecules

The structure of Boc-Tyr-ALUVAL-Acp-OMe (**1**) shown in Figure 3 is very similar to the corresponding portion (upper helix and linker) of Figure 2. The Tyr1 that replaced Val1 has had no particular effect on the helix, despite the formation of a hydrogen bond O(1H)···O(4) with a neighboring helix. The Acp linker, now placed at the C terminus of **1**, has the same conformation as when placed between two L helices, as in Figure 2.

A stereodiagram of the conformation of Boc-L-(VALUVAL)-Acp-D-(VALUVAL)-OMe (**2**) is shown in Figure 4. At first glance it appears to be quite similar to the L,L analog in Figure 2. The desired U-turn at the Acp linker has not been achieved. In both the L,L and L,D analogs, the axes of the upper and lower helices are displaced from each other laterally but still remain pointed in the same direction, rather than in an antiparallel direction that would result in a two-helix bundle.

The upper helices in the L,L and L,D analogs have nearly identical conformations, as can be ascertained by comparing the $\phi$ and $\psi$ values for torsional angles, the intramolecular 4→1 and 5→1 hydrogen bonds and the least-squares fit where the average deviation for the 33 backbone and $C^{\beta}$ atoms (C1A to C7′) is 0.25 Å (see the left-hand side of Figure 5). The lower helices in the L,L and L,D analogs are also quite similar except for handedness. The L helix has negative $\phi$ and $\psi$ values. Furthermore, the L helix is right handed while the D helix is left handed.

The main difference between the L,L and L,D analogs lies in the different orientation of the lower helix with respect to the upper helix as is illustrated in Figure 5. This difference is correlated with the different conformation of the Acp linker in the two analogs. In the L,L analog the pentamethylene chain in Acp is extended, as compared to the L,D analog where the pentamethylene moiety assumes a helical form with torsional angles near –50° or –60°.

**Figure 4**

Stereodiagram of two molecules of Boc-L-(VALUVAL)-Acp-D-(VALUVAL)-OMe (**2**). The Acp linker is shown as filled circles. The upper helix (L) is right handed while the lower helix (D) is left handed. Two hydrogen bonds N9···O6a and N10···O7a link the upper helix of one molecule with the lower helix of the adjacent molecule.

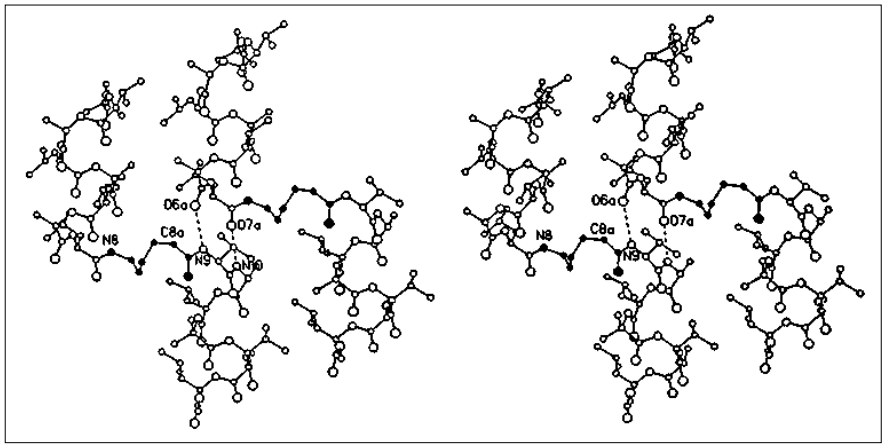

**Figure 5**

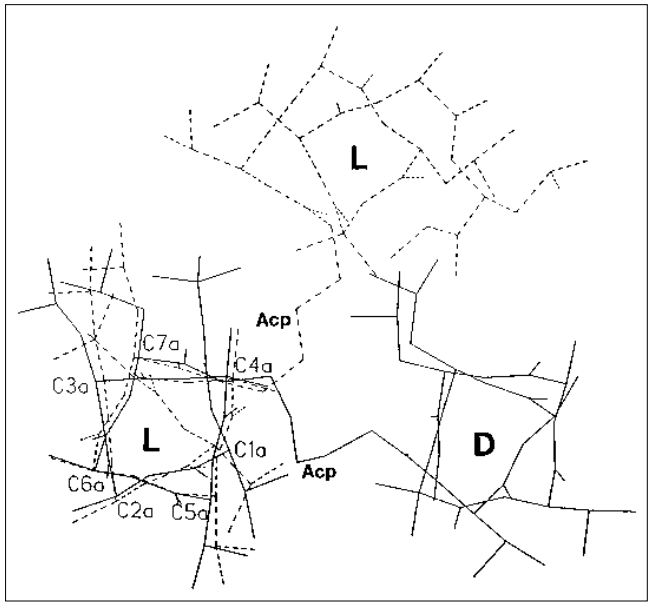


Comparison of the L,L peptide (dashed lines) with the L,D peptide (solid lines). The view is from the top looking into the helices. The least-squares fit was made with the upper L helices of the two analogs. The Acp linker is extended in the L,L peptide and helical in the L,D peptide.

**Figure 6**

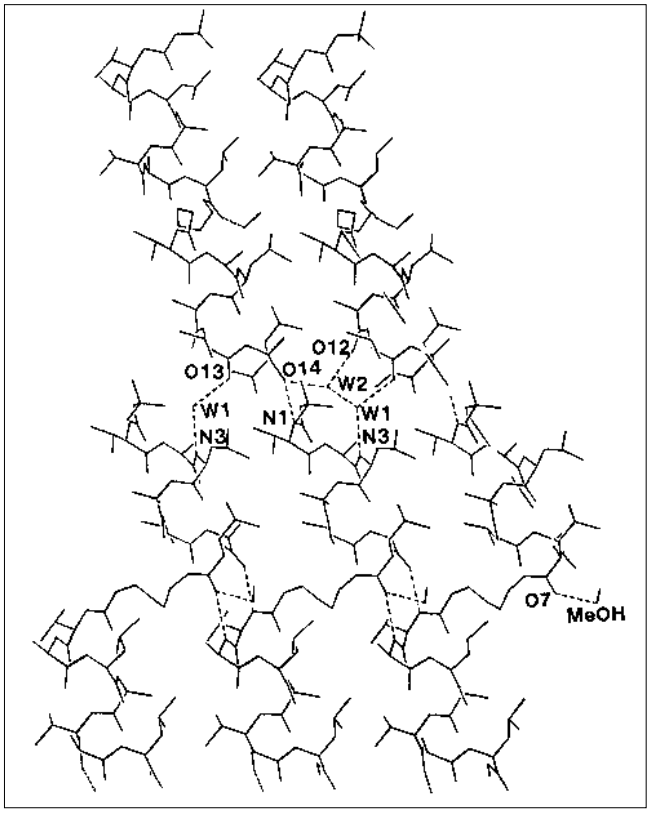


Two layers of helix–linker–helix hydrogen-bonded ribbons. The upper layer is rotated 90° (about the vertical direction) with respect to the lower layer. Between the layers dashed lines indicate head-to-tail hydrogen bonds. Within the layers dashed lines indicate hydrogen bonds shown in Figure 4 and $CH_3OH\cdots O7$ where methanol is co-crystallized with the peptide.

### Molecular assemblies

The assembly of neighboring L,L and L,D molecules in their respective crystals has several similarities. In both crystals, the molecules nestle within each other in the lateral direction so that a pair of intermolecular hydrogen bonds, N(9)H···O(6) and N(10)H···O(7), link the upper helix of one molecule with the lower helix of the neighboring molecule in such a way that the two helices appear as a continuation of one helix. A repetition of this mode of hydrogen bonding between adjacent molecules forms relatively flat infinite ribbons whose width is the length of one helix–linker–helix molecule. The ability to form the above two hydrogen bonds may be responsible for the preferred conformation of the elongated form of the helix–linker–helix molecule with laterally displaced helices rather than the desired folded two-helix bundle.

The hydrogen-bonded ribbons have NH moieties extending from the tops of the helices and C=O moieties extending from the bottoms of the helices that participate in hydrogen bonds between ribbons. These hydrogen bonds fall into two categories, the direct head-to tail NH···C=O type and the water (or solvent) mediated NH···W···O=C type. Examples of the former in **2** are N(1)H···O(14) and of the latter are:

N(3)—W1—O(13)
|
O(12)—W2—O(14)

Two layers of ribbons in **2** are shown in Figure 6. The lower part of the diagram shows a ribbon approximately in the plane of the paper. The upper part of the diagram shows the ribbons edge-on with a rotation of 90° about the vertical direction. Hence the crystal is composed of four repeating sets of ribbons each rotated by 90° to the set below (or above) that satisfies the fourfold screw rotation of the $P4_1$ space group. Figure 7 shows the relationship of the four symmetry-related molecules along the $z$ axis.

### Conclusions

In the present study, an attempt to construct a compact two-helix bundle motif with antiparallel orientation has been partially successful. The desired orientation between the two helices has not been achieved despite the use of two helical modules of reverse chiral senses connected by a flexible linker. The present investigation also focuses on the conformational property of the flexible linker ϵ-aminocaproic acid residue. It is influenced by the chirality of the helical module(s) with which it is attached. The Acp linker adopts extended conformations when it is

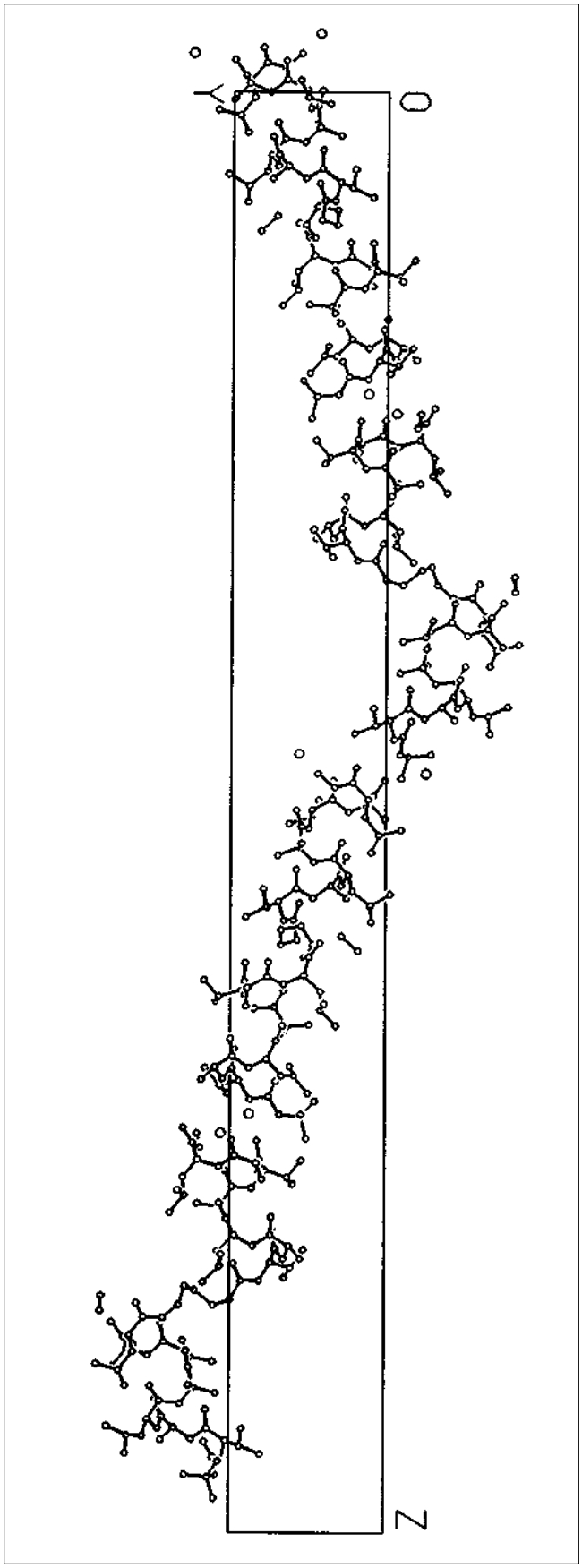

**Figure 7**

Packing of 2 in a spiral in the cell with $P4_1$ symmetry. The ribbons shown in Figures 4 and 6 contain additional molecules related to the molecules in this diagram only by translation in the *x* or *y* directions.

**Table 1**

**Diffraction and crystal parameters for Boc-L-Tyr-L-(ALUVAL)-Acp-OMe (1) and Boc-L-(VALUVAL)-Acp-D-(VALUVAL)-OMe (2).**

| | 1 | 2 |
|---|---|---|
| Empirical formula | $C_{48}H_{80}N_8O_{12}\cdot H_2O$ | $C_{77}H_{145}N_{15}O_{21}\cdot 2H_2O\cdot MeOH$ |
| Crystallizing solvent | $MeOH/H_2O$ | $MeOH/H_2O$ |
| Color/habit | Soft, sticky | Colorless, square plates |
| Crystal size (mm) | 0.20×0.30×0.60 | 0.20×0.20×0.35 |
| Space group | $P2_12_12_1$ | $P4_1$ |
| Cell parameters | | |
| *a* (Å) | 11.094(2) | 10.094(6) |
| *b* (Å) | 18.455(4) | 10.094(6) |
| *c* (Å) | 27.625(5) | 93.383(12) |
| Volume (Å$^3$) | 5655.94 | 9514.69 |
| *Z* | 4 | 4 |
| Formula weight | 961.2 | 1609.0 |
| Density (calc'd) (g/cm$^3$) | 1.129 | 1.123 |
| F(000) | 2080 | 3520 |
| Temperature | 21°C | 21°C |
| Crystal mounting | Dry | Dry |
| Radiation, λ (Å) | $CuK_\alpha$, 1.54178 | $CuK_\alpha$, 1.54178 |
| 2θ range (deg) | 3–114 | 3–114 |
| Resolution (Å) | 0.93 | 0.93 |
| Scan type | θ/2θ | Omega |
| Scan speed (deg/min) | 10 | 10 |
| Scan range | 2° plus $K_\alpha$ separation | 2° plus $K_\alpha$ separation |
| Index range | | |
| *h* | 0 to 12 | –5 to +8 |
| *k* | 0 to 20 | 0 to +10 |
| *l* | 0 to 30 | 0 to +100 |
| Independent refls | 4325 | 5824 |
| Obs'd refls $\lvert F_o \rvert > 3\sigma(F)$ | 2655 | 3668 |
| Final R indices (%) (observed data) | 7.30 | 7.15 |
| Final $R_w$ indices (%) (observed data) | 6.49 | 6.35 |
| Weight | 0.00025 | 0.00025 |
| *S* | 1.68 | 1.65 |
| No. parameters refined | 626 | 1018 |
| Data : parameter ratio | 4.2:1.0 | 3.6:1.0 |
| Largest difference peak (eÅ$^{-3}$) | 0.24 | 0.24 |
| Largest difference hole (eÅ$^{-3}$) | –0.21 | –0.27 |

**Table 2**

**Torsional angles*† for Boc-L-Tyr-L-(ALUVAL)-Acp-OMe (1).**

| | $\phi$ | $\psi$ | $\omega$ | $\chi^1$ | $\chi^2$ | $\theta_2$ | $\theta_1$ |
|---|---|---|---|---|---|---|---|
| Tyr1 | –55 | –45 | –178 | 176 | 83, –98 | | |
| Ala2 | –58 | –38 | +177 | | | | |
| Leu3 | –70 | –43 | +178 | –177 | –175, 58 | | |
| Aib4 | –52 | –47 | –176 | | | | |
| Val5 | –76 | –38 | +180 | –61, 173 | | | |
| Ala6 | –67 | –28 | +177 | | | | |
| Leu7 | –76 | –35 | –171‡ | –73 | 173, –62 | | |
| Acp8# | +94§ | +94 | –169 | –21($\theta_4$) | –164($\theta_3$) | +173($\theta_2$) | –70($\theta_1$) |

*The torsion angles for rotation about bonds of the peptide backbone ($\phi$,$\psi$,$\omega$) and bonds of the amino sidechains ($\chi^n$) are described in [6]. †Esd's ~1.0. ‡$C^\alpha$(7), C′(7), N(8), $C^\epsilon$(8). §C′(7), N(8), $C^\epsilon$(8), $C^\delta$(8). #Torsions in the mainchain in the linker Acp about $C^\alpha$–$C^\beta$, $C^\beta$–$C^\gamma$, $C^\gamma$–$C^\delta$ and $C^\delta$–$C^\epsilon$ are designated $\theta_4$ to $\theta_1$, respectively. In ω-amino acids, the N–$C^\omega$ bond is designated as $\phi$, the $C^\alpha$–CO bond as $\psi$, while the remaining C–C dihedrals are denoted as $\theta_1$, $\theta_2$··· beginning from the N-terminal end.

linked to either an L helix or a pair of L helices, while it adopts a nearly helical conformation when it is attached to an L,D helix pair. The use of stereochemically defined rigid linking segments and the introduction of additional specific interhelix interaction between the two helical modules merit further investigation.

## Materials and methods

### *Peptide synthesis*

Peptides were synthesized by conventional solution phase methods [34] by using a racemization free fragment condensation strategy. The Boc group was used for N-terminal protection and the C terminus was protected as a methyl ester. Deprotections were performed using 98% formic acid or saponification, respectively. Couplings were mediated by dicyclohexylcarbodiimide-1-hydroxybenzotriazole (DCC/HOBT). Homogeneity of the peptide fragments was regularly checked by thin layer chromatography (TLC) on silica gel using 9:1 $CHCl_3$:$CH_3OH$ as eluant. Fragments larger than 4 residues were checked for homogeneity on a reverse phase C-18 column. All crude peptides were purified by medium pressure liquid chromatography (MPLC) on a C-18 column using aqueous methanol gradients as eluants. The final peptides were further purified by high-performance liquid chromatography (HPLC) on a Lichrosob reverse phase C-18 HPLC column (4 × 250 mm, particle size 10 μ, flow rate 1.5 ml/min) and eluted on a linear gradient of methanol/water (70–95%). All peptides were characterized by HPLC analysis and $^1$H NMR (80 or 400 MHz).

### *X-ray diffraction*

Clear colorless crystals of Boc-L-Tyr-L-(ALUVAL)-Acp-OMe (1) and Boc-L-(VALUVAL)-Acp-D-(VALUVAL)-OMe (2) were grown by slow evaporation from methanol/water (9:1) solution. X-ray data were measured at room temperature with a Siemens P4 automated four circle diffractometer equipped with a graphite monochromator. Diffraction and crystal parameters for 1 and 2 are listed in Table 1. It should be noted that in 2, the *c* axis is >93 Å long. The crystal scattered well to indices of 100 for *l*. In order to collect data to 0.93 Å resolution, the X-ray detector had to be in its usual position, with a distance of 19.5 cm from crystal to detector, which meant that there would be overlap of the edges of the profiles for many of the diffracted spots if the $\theta/2\theta$ scan mode were used. Therefore, the omega scan mode was chosen though it presented other overlap difficulties for some low-angle reflections. A number of these reflections were culled manually and not used in the

**Table 3**

**Hydrogen bonds in Boc-L-Tyr-L-(ALUVAL)-Acp-OMe (1).**

| Type | Donor | Acceptor | O–O or N–O (Å) | H–O (Å)* | C=O···N angle (deg) |
|---|---|---|---|---|---|
| Head-to-tail | N(1) | O(6)† | 2.895 | 2.02 | |
| | N(2) | O(7)† | 2.922 | 2.10 | |
| 4→1 transition | N(3) | O(0) | 3.027 | 2.41 | 128 |
| 5→1 transition | N(4) | O(0) | 3.050 | 2.17 | 158 |
| | N(5) | O(1) | 2.988 | 2.12 | 167 |
| | N(6) | O(2) | 3.081 | 2.26 | 144 |
| | N(7) | O(3) | 2.985 | 2.20 | 160 |
| | N(8)‡ | | | | |
| Sidechain–backbone | O(1H)§ | O(4) | 2.716 | | |
| Water–peptide | W(1)# | O(2) | 2.717 | | |
| | W(1)** | O(1H) | 2.961 | | |

*Hydrogen atoms have been placed in idealized positions with N-H = 0.90 Å. †Symmetry equivalent 1.5–x, 2–y, –0.5+z to coordinates listed in the Cambridge Crystallographic Data File. ‡N(8)···O(5), 3.38 Å; N(8)···O(4), 3.57 Å. §Symmetry equivalent –0.5+x, 2.5–y, –z. #Symmetry equivalent 0.5+x, 1.5–y, –z. **Symmetry equivalent x, 1+y, z. Atom O(8) does not participate in any hydrogen bonding.

**Table 4**

**Torsional angles*† for Boc-L-(VALUVAL)-Acp-D-(VALUVAL)-OMe (2).**

| | $\phi$ | $\psi$ | $\omega$ | $\chi 1$ | $\chi 2$ | $\theta_2$ | $\theta_1$ |
|---|---|---|---|---|---|---|---|
| L-Val1 | –69 | –47 | –176 | 168, –66 | | | |
| L-Ala2 | –64 | –45 | +178 | | | | |
| L-Leu3 | –61 | –42 | +179 | –151 | –177, 33 | | |
| Aib4 | –54 | –49 | –179 | | | | |
| L-Val5 | –61 | –46 | –178 | 169, –66 | | | |
| L-Ala6 | –61 | –38 | –174 | | | | |
| L-Leu7 | –89 | –38 | –161 | –66 | 174, –63 | | |
| Acp8# | –102 | –96 | +175 | –63($\theta_4$) | –53($\theta_3$) | –51($\theta_2$) | –65($\theta_1$) |
| D-Val 9 | +57 | +49 | +177 | –171, +67 | | | |
| D-Ala10 | +62 | +39 | –174 | | | | |
| D-Leu11 | +67 | +39 | +179 | +68 | –176, +62 | | |
| Aib12 | +61 | +27 | –177 | | | | |
| D-Val13 | +78 | +53 | +172 | –170, +68 | | | |
| D-Ala14 | +72 | +40 | –177 | | | | |
| D-Leu15 | +77 | +44 | –179 | +61 | –173, +68 | | |

*The torsion angles for rotation about bonds of the peptide backbone ($\phi$,$\psi$,$\omega$) and bonds of the amino sidechains ($\chi^n$) are described in [6]. †Esd's ~1.0. ‡$C^\alpha$(7), C′(7), N(8), $C^\epsilon$(8). §C′(7), N(8), $C^\epsilon$(8), $C^\delta$(8). #Torsions in the mainchain in the linker Acp about $C^\alpha$–$C^\beta$, $C^\beta$–$C^\gamma$, $C^\gamma$–$C^\delta$ and $C^\delta$–$C^\epsilon$ are designated $\theta_4$ to $\theta_1$, respectively.

structure development. The data yielded a structure with acceptable bond lengths, angles and R factor.

The structures were solved by a vector search procedure contained in the PATSEE computer program [35] contained in the SHELXTL package of programs (Siemens Instruments, Madison, WI). The model used in the search for **1** consisted of 27 backbone and $C^\beta$ atoms – $C^\alpha$(4) to $C^\alpha$(9) — from the known structure of Boc-Gly-Dpg-Pro-Val-Ala-Leu-Aib-Val-Ala-Leu-OMe and for **2** the model consisted of 26 atoms — $C^\alpha$(2) to $C^\alpha$(8) — present in the refined structure of **1**. After using PATSEE to obtain the rotation and translation of the models for **1** and **2** to the correct position in the respective cells, the remainder of the

**Table 5**

**Hydrogen bonds in Boc-L-(VALUVAL)-Acp-D-(VALUVAL)-OMe (2).**

| Type | Donor | Acceptor | N–O or O–O (Å) | H–O (Å)* | C=O···N angle (deg) |
|---|---|---|---|---|---|
| Head-to-tail | N(1) | O(14)† | 2.964 | 2.06 | 141 |
| | N(2) | | | | |
| Peptide–solvent | N(3) | W(1)‡ | 2.979 | 2.11 | |
| 5→1 transition | N(4) | O(0) | 2.920 | 2.07 | 161 |
| | N(5) | O(1) | 3.129 | 2.25 | 155 |
| | N(6) | O(2) | 3.031 | 2.18 | 154 |
| | N(7) | O(3) | 2.900 | 2.07 | 159 |
| | N(8) | O(4) | 2.926 | 2.13 | 157 |
| Interpeptide | N(9) | O(6)§ | 2.939 | 2.07 | 147 |
| | N(10) | O(7)§ | 3.004 | 2.12 | 133 |
| Solvent–peptide | O(1S) | O(7) | 2.717 | | |
| | N(11) | O(1S)§ | 3.276 | 2.43 | |
| 5→1 transition | N(12) | O(8) | 2.859 | 2.02 | 165 |
| | N(13) | O(9) | 3.130 | 2.37 | 155 |
| | N(14) | O(10) | 3.016 | 2.15 | 156 |
| | N(15) | O(11) | 2.824 | 1.95 | 158 |
| Water–peptide | W(2)# | O(12) | 2.946 | | |
| | W(1) | O(13) | 2.890 | | |
| | W(2) | O(14) | 2.790 | | |
| | W(1) | W(2) | 2.895 | | |

*Hydrogen atoms have been placed in idealized positions with N-H = 0.90 Å. †Symmetry equivalent 1–y, x, 0.25+z to coordinates. ‡Symmetry equivalent –y, x, 0.25+z. §Symmetry equivalent 1+x, y, z. #Symmetry equivalent x, –1+y, z.

atoms were found with a procedure based on the partial structure procedure [36]. Full matrix anisotropic least-squares refinement was performed on the C, N and O atoms in the peptides, after which hydrogen atoms were placed in idealized positions, with C-H = 0.96 Å and N-H = 0.90 Å, and allowed to ride with the C or N atom to which each was bonded for the final cycles of refinement. The thermal factor for the hydrogen atoms was fixed at $U_{iso}$ = 0.08. The sidechain in Val5 in **1** is disordered so that there is some occupancy of the two $C^{\gamma}$ atoms in three sites, *gauche*$^{+}$, *gauche*$^{-}$ and *trans* positions (occupancy of each Val5 $C^{\gamma}$ atom site is 0.8, 0.6 and 0.6).

Bond lengths and bond angles (esd's ~ 0.018 Å for bond lengths and ~ 1.0° for angles) do not show significant or systematic differences from expected values. Torsional angles and hydrogen bonds for **1** are shown in Tables 2 and 3, respectively, and for **2** in Tables 4 and 5, respectively.

### *Deposition of coordinates*

Fractional coordinates for C, N and O atoms in **1** and **2**, bond lengths and angles, anisotropic thermal parameters and coordinates for hydrogen atoms will be deposited with the Cambridge Crystallographic Data file. Observed and calculated structure factors are available from IL Karle.

## Acknowledgements

This research was supported in part by a grant from the Department of Science and Technology, India and by the National Institute of Health Grant GM-30902 and the Office of Naval Research.

## References

1. Dill, K.A. (1990). Dominant forces in protein folding. *Biochemistry* **29**, 7133–7155.
2. Richards, F.M. (1991). The protein folding problem. *Sci. Am*. **264**, 54–63.
3. Miranker, A.D. & Dobson, C.M. (1996). Collapse and cooperativity in protein folding. *Curr. Opin. Struct. Biol.* **6**, 31–42.
4. Betz, S.F., Raleigh, D.P. & DeGrado, W.F. (1993). *De novo* protein design: from molten globules to native-like states. *Curr. Opin. Struct. Biol.* **3**,601–610.
5. Richardson, J.S., *et al.*, & Surles, M.C. (1992). Looking at proteins: representation, folding, packing and design. *Biophys. J.* **63**, 1186–1209.
6. Bryson, J.W., *et al.*, & DeGrado, W.F. (1995). Protein design: a hierarchic approach. *Science* **270**, 935–941.
7. Mutter, M., *et al.*, & Rivier, J.E. (1992). Template-assembled synthetic proteins with four-helix-bundle topology. Total chemical synthesis and conformational studies. *J. Am. Chem. Soc.* **114**, 1463–1470.
8. Vulleumiers, S. & Mutter, M. (1993) Synthetic peptide and template assembled synthetic protein models of hen egg white lysozyme 87–93 helix: importance of a protein like frame work for conformational stability in a short peptide sequence. *Biopolymers* **33**, 389–400.
9. Mutter, M., *et al.*, & Tuchscherer, G. (1996). Template assembled synthetic protein (TASP) as functional mimics of proteins. *Angew. Chem. Int. Ed. Engl.* **35**, 1482–1485.
10. Akerfeldt, K.S., Kim, R.M., Camac, D., Groves, J.T., Lear, J.D. & DeGrado, W.F. (1992). Tetraphilin: a four helix proton channel built on a tetraphenylporphyrin framework. *J. Am. Chem. Soc.* **114**, 9656–9657.
11. Ranabal, F., DeGrado, W.F. & Dutton, P.L. (1996). Toward the synthesis of a photosynthetic reaction center maquette: a cofacial porphyrin pair assembled between two subunits of a synthetic four helix bundle multiheme protein. *J. Am. Chem. Soc.* **118**, 473–474.
12. Ghadiri, M.R., Soares, C. & Choi, C. (1992). A convergent approach to protein design. Metal ion-assisted spontaneous self-assembly of a polypeptide into a triple-helix bundle protein. *J. Am. Chem. Soc*. **114**, 825–831.
13. Lieberman, M. & Sasaki, T. (1991). Iron (II) organizes a synthetic peptide into three helix bundles. *J. Am. Chem. Soc.* **113**, 1470–1471.
14. Regan, L. (1995). Protein design: novel metal-binding sites. *Trends Biochem. Sci.* **20**, 280–285.
15. Hecht, M.H., Richardson, J.S., Richardson, D.C. & Ogden, R.C. (1990). *De novo* design, expression, and characterization of Felix: a four-helix bundle protein. *Science* **249**, 884–891.
16. Regan, L., Rockwell, A., Wasserman, Z. & DeGrado, W.F. (1993) Disulfide crosslink to probe the structure and flexibility of a designed four helix bundle protein. *Protein Sci.* **3**, 2419–2427.
17. Predki, P.F. & Regan, L. (1995). Redesigning the topology of a four helix bundle protein: monomeric rop. *Biochemistry* **34**, 9834–9839.
18. Raleigh, D.P., Betz, S.F. & DeGrado, W.F. (1995). A *de novo* designed protein mimics the native state of natural proteins. *J. Am. Chem. Soc.* **117**, 7558–7559.
19. Karle, I.L., Flippen-Anderson, J.L., Sukumar, M., Uma, K. & Balaram, P. (1991). Modular design of synthetic protein mimics. Crystal structure of two seven-residue helical peptide segments linked by ε-aminocaproic acid. *J. Am. Chem. Soc.* **113**, 3952–3956.
20. Karle, I.L., Awasthi, S.K. & Balaram, P. (1996). A designed β-hairpin peptide in crystals. *Proc. Natl. Acad. Sci. USA* **93**, 8189–8193.
21. Balaram, P. (1992). The design and construction of synthetic protein mimics. *Pure Appl. Chem.* **64**, 1061–1066.
22. Karle, I.L., Flippen-Anderson, J.L., Uma, K., Sukumar, M. & Balaram, P. (1990). Modular design of synthetic protein mimics. Structures, assembly and hydration of two 15 and 16 residue apolar helical peptides in crystals. *J. Am. Chem. Soc*. **112**, 9350–9356.
23. Karle, I.L., Gurunath, R., Prasad, S., Kaul, R., Rao, R.B. & Balaram, P. (1995). Peptide design. Structural evaluation of potential non-helical segments attached to helical modules. *J. Am. Chem. Soc.* **117**, 9632–9637.
24. Karle, I.L., Rao, R.B., Prasad, S., Kaul, R. & Balaram, P. (1994). Nonstandard amino acids in conformational design of peptides. Helical structures in crystals of 5–10 residue peptides containing dipropylglycine and dibutylglycine *J. Am. Chem. Soc.* **116**, 10355–10361.
25. Banerjee, A., Datta, S., Pramanik, A. & Balaram, P. (1996). Heterogeneity and stability of helical conformations in peptides: crystallographic and NMR studies of a model heptapeptide. *J. Am. Chem. Soc.* **118**, 9477–9483.
26. Karle, I.L., Kishore, R., Raghothama, S. & Balaram, P. (1988). Cyclic cystine peptides. Antiparallel beta-sheet conformation for the 20-membered ring in Boc-Cys-Val-Aib-Ala-Leu-Cys-$NHCH_3$. *J. Am. Chem. Soc.* **110**, 1958–1963. S----------S
27. Awasthi, S.K., Raghothama, S. & Balaram, P. (1995). A designed β-hairpin peptide. *Biochem. Biophys. Res. Commun.* **216**, 375–381.
28. Bryant, J.A., Ericson, J.L. & Cram, D.J. (1990). High preorganization of large lipophilic surfaces common to two complexing partners provides high binding energies that vary dramatically with changes in organic solvent composition. *J. Am. Chem. Soc.* **112**, 1255–1256.
29. Whitesides, G.M., *et al.*, & Gordon, D.M. (1995). Noncovalent synthesis: using physical-organic chemistry to make aggregates. *Acc. Chem. Res.* **28**, 37–44.
30. Karle, I.L. & Balaram, P. (1990). Structural characteristics of α-helical peptide molecules containing Aib residues. *Biochemistry* **29**, 6747–6756.
31. Prasad, B.V.V. & Balaram, P. (1984) The stereochemistry of α-aminoisobutyric acid containing peptides. *CRC Crit. Rev. Biochem*. **16**, 307–347.
32. Uma, K., Karle, I.L. & Balaram, P. (1991). Towards the design of structural mimics for proteins using helical peptide modules. In *Proteins: Structure, Dynamics and Design.* (Renugopalakrishnan, V., Carey, P.R., Smith, I.C.P., Huang, S.G. & Storer, A., eds.) pp. 295–301, Escom Science Publishers B.V., Leiden.
33. Gurunath, R. & Balaram, P. (1994). Incorporation of a potentially helix breaking D-Phe-Pro sequence into the center of a right handed 16-residue peptide helix. *Biochem. Biophys. Res. Commun.* **202**, 241–245.
34. Balaram, H., Sukumar, M. & Balaram, P. (1986). Stereochemistry of α-aminoisobutyric acid peptides in solution. Conformations of decapeptides with a central triplet of contiguous L-amino acids. *Biopolymers*. **25**, 2209–2223.
35. Egert, E. & Sheldrick, G.M. (1985). Search for a fragment of known geometry by integrated Patterson and direct methods. *Acta. Crystallogr. A* **41**, 262–268.
36. Karle, J. (1968). Partial structure information combined with the tangent formula for noncentrosymmetric crystals. *Acta. Crystallogr. B* **24**, 182–186.